University of Salerno

Department of Information and Electrical Engineering and Applied Mathematics

Master Degree in Computer Engineering

IDL implementations of HPF, GIHS and Brovey algorithms for Pansharpening

Remote Sensing

A.A. 2023/2024

Group A:

Carrozza Franscesco, mat.: 0622702061
Ciaravolo Ciro, mat.: 0622702006
Marcone Giuseppe, mat.: 0622701896
Pepe Lorenzo, mat.: 0622702121

Index

Introduction

This report summarizes all the work done for the exam of Remote Sensing held by Paolo Addesso, of University di Salerno, within the Embedded Systems specialization of the Department of Information and Electrical Engineering and Applied Mathematics, in the academic year 2023/2024. The report will introduce first a general view of the examination subject, with a focus on the pan-sharpening technique. Then the main arguments of the project work will be described, with special attention on the three algorithms of pan-sharpening developed in the IDL language: a brief introduction for each algorithm, to explain the different approach to the problem, then the implementation in IDL and Envi. Final the results will be discussed, either through visually confront the pan-sharpened image with the ground truth and the full-scale multispectral images and using specific quality indexes (SAM, ERGAS, Q2N).

The work described in this paper has seen the combined work of the four students to implements the three algorithms in IDL and to provide an Envi interface to facilitate the input of images and the choice of algorithm to be used.

1 A brief introduction to the Remote Sensing

In a general view, remote sensing refers to the acquisition of information about an object of phenomena without making physical contact with the object, or phenomena, observed. The term is applied specially to acquiring information about the Earth and other planets. It’s applied to various fields: hydrology, ecology, meteorology, oceanography, glaciology, geology. It also has military, intelligence, commercial, economic, planning, and humanitarian applications, among others.

In current usage, the term remote sensing generally refers to the use of satellite- or aircraft-based sensor technologies to detect and classify objects on Earth. It includes the surface and the atmosphere and oceans, based on propagated signals (e.g. electromagnetic radiation). It may be split into "active" remote sensing (when a signal is emitted by a satellite or aircraft to the object and its reflection is detected by the sensor) and "passive" remote sensing (when the reflection of sunlight is detected by the sensor).

The subject matter spans several areas: physics and electronics, embedded system and sensors development, data analysis and telecommunication, and, in modern days, machine learning and AI. As can be understood the acquisition and analysis of image from satellite is a multi-disciplinary effort.

1.2 Passive and active remote sensing

Passive remote sensing exploits the reflection of sun light from earth surface and atmosphere. Sensors, placed on satellite platform at various height, detect such light and send back data to the ground stations with the image splits in various spectral bands (depending on the sensor). Images detected from passive sensors are used in this project.

Active remote sensing makes use of sensors such as radar, lidar or SAR (Synthetic Aperture Radar). The main difference consists in the fact that the sensors does not require an “external” source of light or sound wave, but the sensor itself produces the signal that is then reflected from the object back to the sensor.

Advantages for active sensors include the ability to obtain measurements anytime, regardless of the time of day or season. Passive sensor advantages are that they consume less power, generating less noise, since they do not require an external source of power to generate the signal.

1.3 Spectrum of images and data characteristics

As said before, received data is split into various bands. The number of bands received depends on the sensor used. Typically, modern sensors acquire at least images in the visible bands (RGB), spacing from nm to nm of the wavelength.
Received data quality is based on four values:

1. *Spatial Resolution*: the size of a pixel that is recorded in a raster image – typically pixels may correspond to square areas ranging in side-length from 1 to 1,000 meters;

2. *Spectral Resolution*: the wavelength of the different frequency bands recorded – usually, this is related to the number of frequency bands recorded by the platform;

3. *Radiometric Resolution*: the number of different intensities of radiation the sensor can distinguish. Typically, this ranges from 8 to 14 bits, corresponding to 256 levels of the gray scale and up to 16,384 intensities or "shades" of color, in each band. It also depends on the instrument noise;

4. *Temporal Resolution*: the frequency of flyovers by the satellite, or plane, and is only relevant in time-series studies or those requiring an averaged or mosaic image as in deforesting monitoring.

1.4 Data fusion and Pan-sharpening

One of the most used techniques in remote sensing is the Data Fusion: the process of integrating multiple data sources to produce more consistent, accurate, and useful information than that provided by any individual data source. An application of data fusion is the technique called Pan-Sharpening. The process uses two identical images, one multispectral, with a low resolution or blurred, (typically RGB, but more bands can be used) and one panchromatic. Then the algorithm extract edge-features from the panchromatic images and apply them on each band of the multispectral image, resulting in a new image with all the features from the original images: a multispectral image with a better resolution.
Many algorithms exist for this technique, but only three will be discussed in this paper: High Pass Filter (HPF), Brovey and GIHS (Generalized Intensity Hue Saturation).

2. Algorithms implemented

2.1 Image rescaling

A portion of the code present in each algorithm implemented deals with the rescaling of images: in the case of a multispectral image with different dimensions from the panchromatic image (a smaller multispectral image), this image is upscaled to match the exact proportion of the panchromatic one. The code utilizes the "*CONGRID*" IDL function.
The results obtained seems identical to the naked eye, but zooming in reveals some artefacts that affect, albeit in the slightest, the values obtained computing the quality indexes. Some examples of these artefacts are visible in Figure 1.

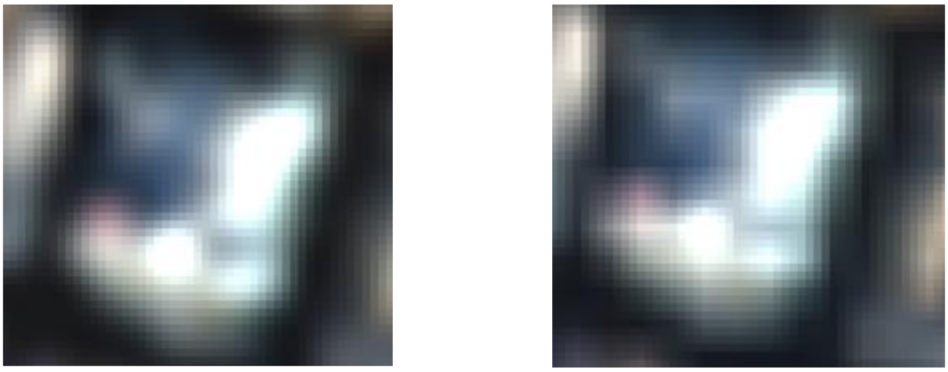

Figure 1 - a) Original low resolution MS detail b) The same MS detail from the upscaled image

Notice how some contour, of the upscaled image on the right, results more demarcated compared to the original multispectral, visible on the left. These effects afflict the output images; however, the results are still like the indexes computed with the images fused without rescaling, so the rescaling can be used in borderline cases or when a multispectral image with the same dimension of a panchromatic image is not available.

2.2 High Pass Filter

The HPF apply a filter to the panchromatic image to extract the edge features to apply on the multispectral image.
The algorithm applies a "Low Pass Filter" to the panchromatic, which extract the surfaces between the edges. Then the edge features are extract subtracting these features to the original panchromatic, obtaining the HPF panchromatic image.
Out algorithm implements this approach in IDL. The low pass filter is applied to the panchromatic image through the "SMOOTH" function, with a kernel size based on the ground sampling distance of panchromatic and multispectral image, based on the formula seen in (1).
As suggested in the paper above, the filter size is calculated as a square window "*N x N*", where:

$$N = (2r + 1),$$
$$r = \frac{GSD_{MS}}{GSD_{PAN}}.$$

The value is passed to the IDL function, which apply the Low Pass Filter. The algorithm then proceeds unaltered.

2.2.1 HPF algorithm translation from MATLAB

Another implementation of the HPF algorithm has been done by translating the MATLAB code to IDL. The MATLAB code is present in (2). The algorithm is more complicated than the previous implementation and involves the computation of mean and standard deviations of both the images and for each multispectral band.
The panchromatic image is then normalized to the multispectral one, and then a low pass filter is applied to the panchromatic image. The algorithm then follows as the previous one.

2.3 Generalized Intensity Hue Saturation

The IHS pansharpening method, exploits the transformation into the IHS color space that mimics the human visual system in processing the intensity (I), hue (H), and saturation (S) information. The IHS transform can be only applied to RGB true color images, leading to a major limitation for processing multispectral images. The GIHS is the generalization of the IHS algorithm, applied to more than three bands.
The IDL implementation uses the same rescaling, if necessary, described in 2.1. Then mean and standard deviations for both images are computed for equalization of the panchromatic image.
The intensity value is subtracted from the equalized panchromatic, obtaining the spatial information of the image. This information is the fused on each band of the multispectral image. The equation used are shown subsequently:

$$D = PAN_{Image} - I,$$
$$OutputMs_{Image} = MS_{LowRes} + D\ ,$$

where $I = mean(MS_{LowRes})$, is the mean calculated on the multispectral image.

2.4 Brovey algorithm

Brovey algorithm for pansharpening exploits a similar way of fusing image as GHIS. As always, the rescaling code described in 2.1 is present in this function. After the resizing, means and standard deviations are computed for all the images.
A very large value, called “*ratio*”, is then computed and used as multiplication factor in the fusion of each band. The equation used are the following:

$$ratio = \frac{PAN\_Image}{(I + \varepsilon)},$$
$$OutputMS_{Image} = MS_{LowRes} * ratio\ ,$$

where $I = mean(MS_{LowRes})$, is the mean calculated on the multispectral image and ε is a very small number.

2.5 Envi interface and other parameters

An interface for Envi has been developed, providing an easy access to the three algorithms. The interface is accessible in the Envi menu, positioned as the last item in the menu, under the name "My Menu". The dropdown menu in Figure 2 shows only one voice called "Pansharpening" which open the interface in Figure 3.

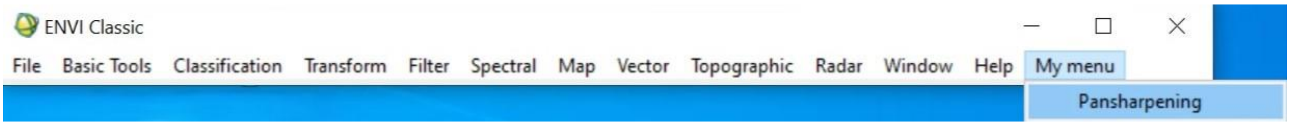

Figure 2 - Envi added menù

From this panel the user can upload the multispectral and panchromatic images, choose the algorithm to use for the fusion and, if necessary, specify the GSD for each band.

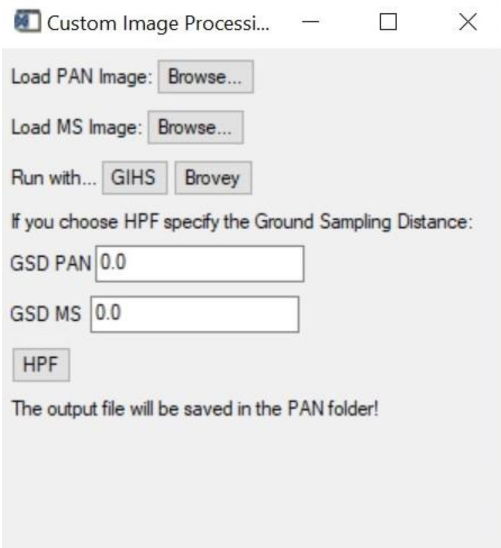

Figure 3 - Envi interface

If the GSD is zero, not specified, a negative number or a value major than 30 (that is the GSD for the low-resolution sensor available on Landsat mission) the kernel size applied for the low pass filter in the HPF function is set to 5. This is a value chosen after some testing, providing a kernel not too small.
The ground sampling distance is an easily found value, being provided in most of the datasheet of the satellite platform. PAirMax GSDs, along with other useful values, were consulted in the table provided in (2), reported here for simplicity.

Image name	Satellite	GSD	*B*	*Q*	Location	Land cover type	Coords. Fig. 3
Pl_Hous_Urb	PHR1B	0.70m PAN, 2.80m MS	4	12	Houston, US	Miscellaneous urban	A1 - A2
W3_Muni_Urb	WV-3	0.31m PAN, 1.24m MS	8	11	Munich, Germany	Dense urban	A3 - A4
GE_Lond_Urb	GE-1	0.46m PAN, 1.84m MS	4	11	London, UK	Urban with long shadows	B1 - B2
W3_Muni_Nat	WV-3	0.31m PAN, 1.24m MS	8	11	Munich, Germany	Agricultural fields and forested areas	B3 - B4
W4_Mexi_Urb	WV-4	0.31m PAN, 1.24m MS	4	11	Mexico City, Mexico	Urban	C1 - C2
S7_Napl_Urb	SPOT-7	1.50m PAN, 6.00m MS	4	14	Naples, Italy	Dense urban, with vegetated areas	C3 - C4
W4_Mexi_Nat	WV-4	0.31m PAN, 1.24m MS	4	11	Mexico City, Mexico	Vegetation and water	D1 - D2
S7_NewY_Mix	SPOT-7	1.50m PAN, 6.00m MS	4	14	New York, US	Urban with water	D3 - D4
W2_Miam_Mix	WV-2	0.46m PAN, 1.84m MS	8	11	Miami, US	Urban with water	E1 - E2
GE_Tren_Urb	GE-1	0.46m PAN, 1.84m MS	4	11	Trenton, US	Heterogeneous urban	E3 - E4
W2_Miam_Urb	WV-2	0.46m PAN, 1.84m MS	8	11	Miami, US	Urban	F1 - F2
Pl_Sacr_Mix	PHR1B	0.70m PAN, 2.80m MS	4	12	Sacramento, US	Urban with water and vegetation	F3 - F4
W3_Muni_Mix	WV-3	0.31m PAN, 1.24m MS	8	11	Munich, Germany	Urban and vegetated areas	G1 - G2
Pl_Stoc_Urb	PHR1B	0.70m PAN, 2.80m MS	4	12	Stockholm, Sweden	Urban	G3 - G4

Figure 4 - GSD and other parameters for PAirMax

3 Visual comparison

In this chapter will be provided all the images fused with the three algorithms, along with the ground truth and the original multispectral full resolution image and panchromatic image, for both the chosen dataset.

3.1 GeoEye-1 London Urban

The first batch show the images fused using the GeoEye-1 dataset taken on the urban zone of London at reduced resolution, using multispectral extended (*b*, *c* and *d*) and low resolution upscaled in IDL (*e*, *f*, and *g*). The first image (*a*) represents the ground truth (GT).

HPF ***GIHS*** ***Brovey***

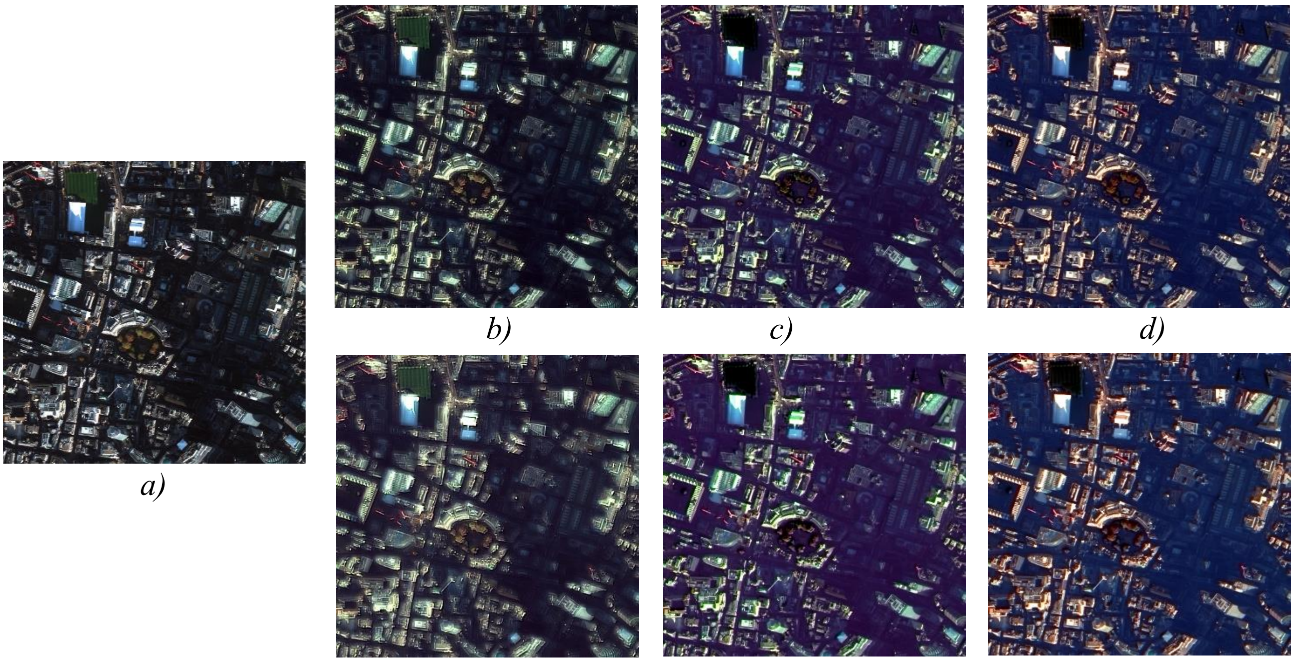

a) *b)* *c)* *d)* *e)* *f)* *g)*

Results for this dataset are excellent with all the algorithms being able to nearly perfectly rebuild the real image, from a blurred one. Some flaws can be seen by the naked eye: HPF tends to somehow give more weight the green band, GIHS instead enhance the blue band while with Brovey the red band seem more dominant. HPF seems to have some trouble fusing rescaled image, while the other two algorithms have similar output relative to the fusion with image not rescaled.

The second batch shows the fused images using the same dataset at full resolution, on the same scene of London.

HPF ***GIHS*** ***Brovey***

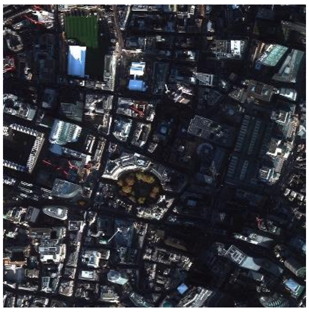

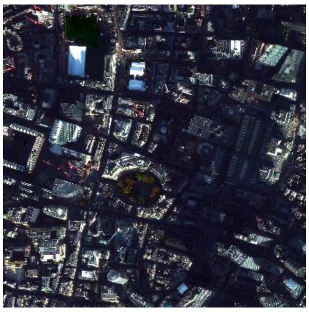
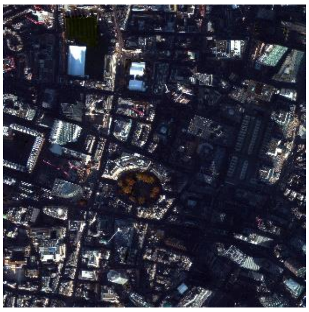

a) *b)* *c)* *d)*




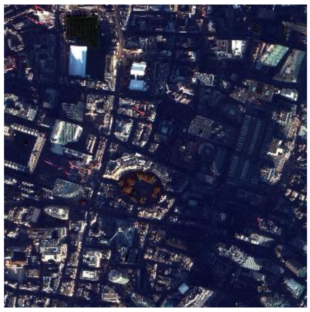

e) *f)* *g)* *h)*

Images *a)* and *e)* represent respectively the expected full resolution multispectral image and the original panchromatic image. As before, the first row (*b*, *c* and *d*) of images are the ones fused with each algorithm using full scale multispectral image, while the second row (*f*, *g* and *h*) are the images fused using the multispectral scaled image, upscaled to match the panchromatic image.

Results with full scale MS image are once again excellent, while persists the same color enhanced effect. Overall, all the output the images have a great improvement in terms of definition, meaning that all the algorithms are working as intended.

3.2 Worldview W4 Mexico Nature

The next dataset considered is the PAirMax Worldview W4, which provide images of Mexican nature. As for the London dataset, the first batch of images for the Worldview W4 will show the image fused using the multispectral extended. The first row (images *b*, *c* and *d*) shows images fused utilizing each algorithm using reduced resolution of the full-scale multispectral images.
The second row (images *e*, *f* and *g*) shows images fused using a reduced resolution downscaled multispectral image, upscaled in IDL to match the panchromatic dimensions.
Image *a* show the ground truth.

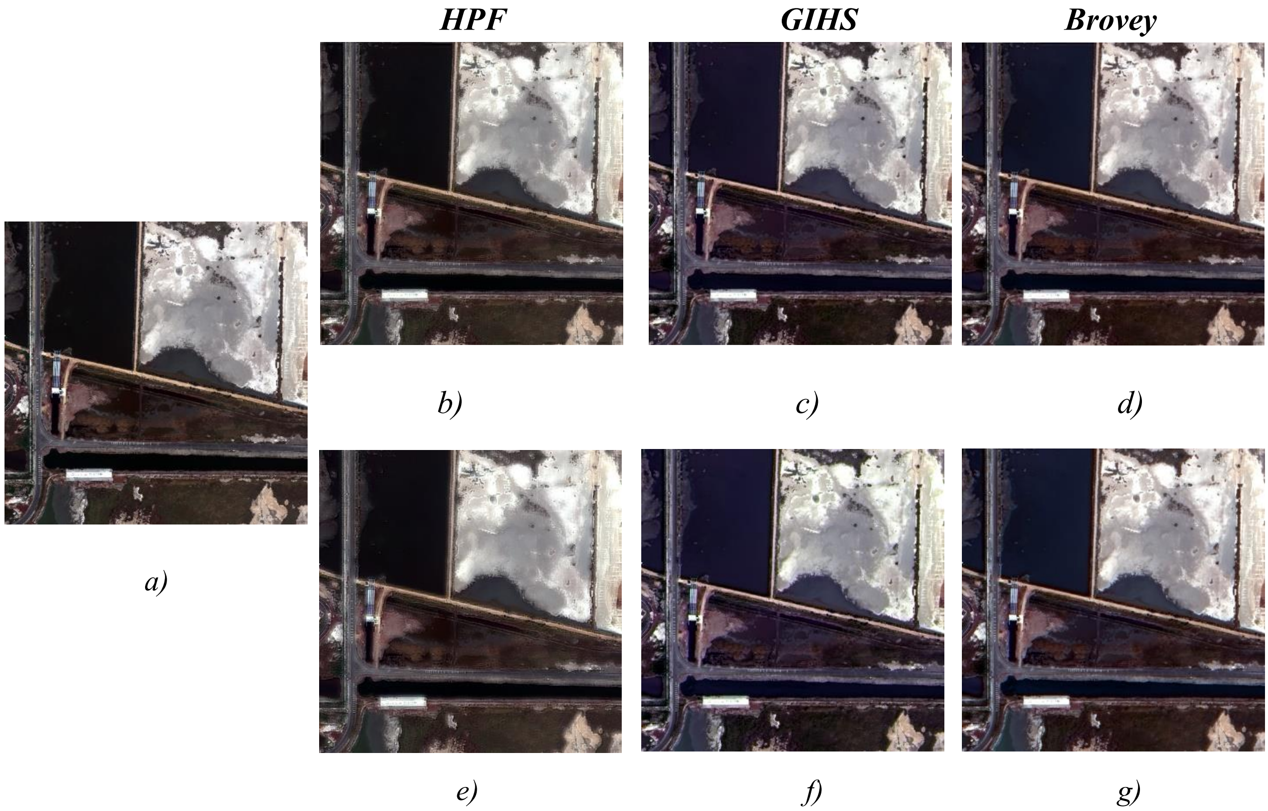

Mexican nature dataset confirms again that the algorithms are working correctly, with a more uniform output between all the combination of algorithm/input image; still the same color effect persists, validating that it is indeed the algorithm that create this effect and not the input images. However, results are excellent in this case too.

The second batch shows imaged fused using the full resolution dataset of the Worldview W4. Same as the London dataset, images *a* and *e* show the expected multispectral image and the original panchromatic image.

HPF ***GIHS*** ***Brovey***

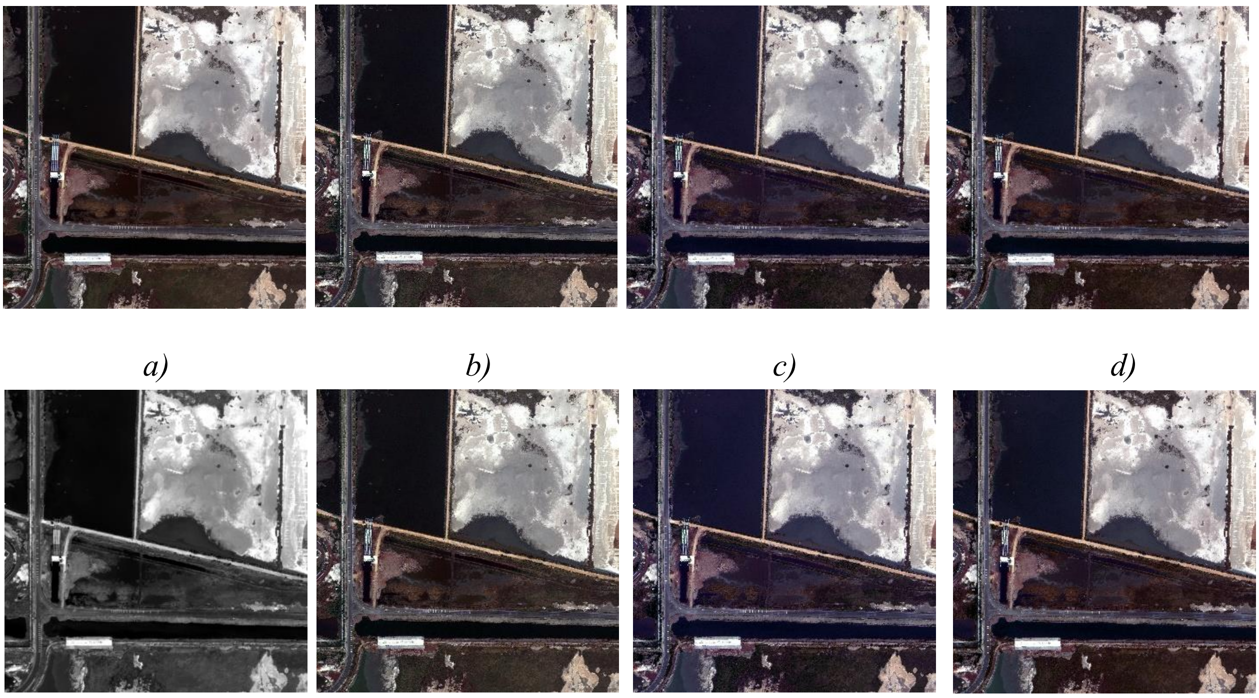

a) *b)* *c)* *d)*

e) *f)* *g)* *h)*

As usual, the first row shows image fused using a full-scale multispectral image, while the second row shows image fused using downscaled multispectral images; image *a* show expected full resolution multispectral image and image *e* show the original panchromatic image.

Results are about the same, as expected, as the London dataset. Again, the color mishap effect persists, but the image quality, in terms of definition, is greatly increased.

4 Quality indexes

Quality indexes are the tool for judging the output images seemingly identical. There are many indexes, but in this course only three will be used.

4.1 Spectral Angle Mapper (SAM) index

The SAM (Spectral Angle Mapper) index is a method used in remote sensing to classify and analyze spectral data. It is particularly useful for hyperspectral imaging, where the goal is to identify and map different materials based on their spectral properties. The SAM index measures the similarity between two spectral signatures by calculating the angle between them in a multidimensional space.
The SAM index is expressed in radians. A smaller angle indicates a higher similarity between the spectral signatures, meaning the target pixel is more likely to be the same material as the reference spectrum.
SAM values can range from 0 to virtually infinite positive values, where a low value means a better image relative to this index.

4.2 Ergas index

The ERGAS (Erreur Relative Globale Adimensionnelle de Synthèse) index is a quantitative metric used to assess the quality of fused or pan-sharpened images in remote sensing. The index measures the overall relative error between a fused image and its reference (typically a higher resolution image). It is widely used to evaluate the quality of image fusion processes, ensuring that the spectral and spatial information from different sources is combined effectively.
It provides a global measure of distortion introduced by the image fusion process. A lower ERGAS value indicates better quality of the fused image, with less distortion and better preservation of original spectral information.
Similarly to SAM, ERGAS values can range from 0 to infinite, where a lower value means a better image relative to this index.

4.3 Q2N index

The Q2N index, or the Universal Image Quality Index for N bands, is an extension of the Universal Image Quality Index (UIQI) tailored for evaluating the quality of multi-band or hyperspectral images. It provides a single quality score by averaging the quality indices of all individual bands, offering a comprehensive assessment of the overall image quality.
It evaluates the similarity between a reference image and a test image across multiple spectral bands, assessing both the spatial and spectral fidelity.
The range of value for this index span from 0 to 1, where low values indicate a poor image quality and high values, close to 1, indicate a good image quality, respectively to the reference image.

For both datasets, these three indexes have been calculated for all the images forged with the three algorithms. The reference for the reduced resolution images is the ground truth, while for the full resolution dataset only a visual comparison has been done.

4.4 Indexes for the GeoEye-1 London urban dataset

The first indexes are computed using the reduced resolution dataset and the low resolution multispectral, at 128x128px, upscaled in IDL.Table 1 summarizes the indexes with the output images from IDL. The algorithms have been implemented following the papers (1) and (2).

Algorithm	SAM	ERGAS	Q2N
HPF	4.8052	30.4121	0.8849
Brovey	4.9106	35.0254	0.7788
GIHS	5.1893	34.0002	0.7874

Table 1 - Indexes for London image, fused with MS upscaled

Table 2 provide the indexes for the images computed with the same dataset but using the blurred 512x512px multispectral image.

Algorithm	SAM	ERGAS	Q2N
HPF	4.0003	25.5388	0.9133
Brovey	4.1973	31.8140	0.8039
GIHS	4.4847	31.1424	0.8121

Table 2 - Indexes for London image, fused with same size PAN and MS

Indexes maps are provided for both the tables. Images *a* and *d* refer to HPF, *b* and *e* refer Brovey, *c* and *f* to GIHS, relative to indexes in the first table.

Table 1

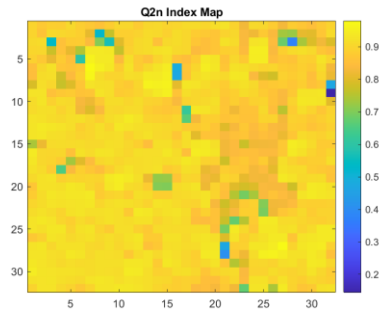

a)

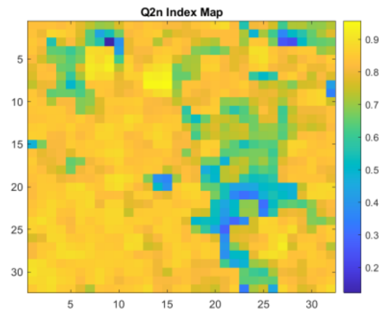

b)

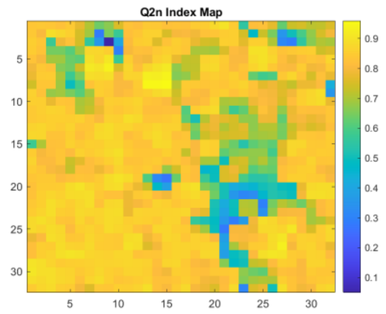

c)

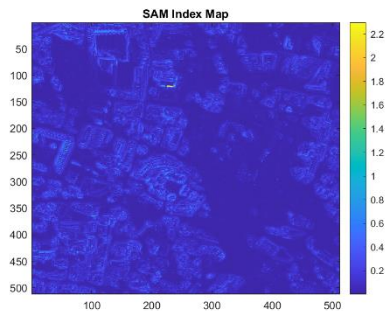

d)

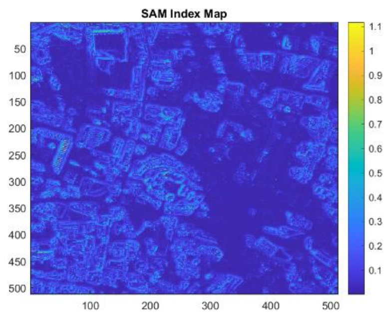

e)

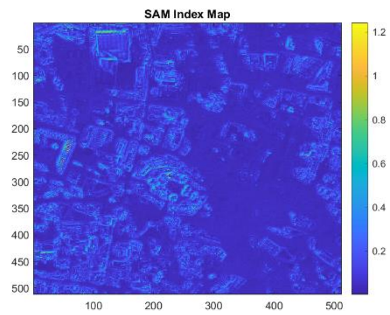

f)

The same scheme is used for displaying the maps for the indexes in Table 2: maps in the first column refers to HPF algorithm, second column refers to Brovey algorithm and the third column refers to GIHS algorithm.

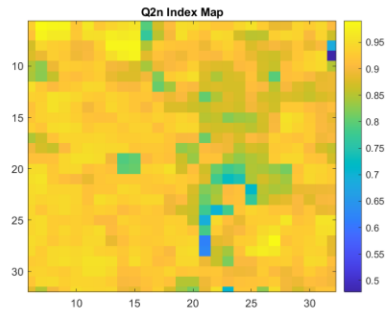

a)

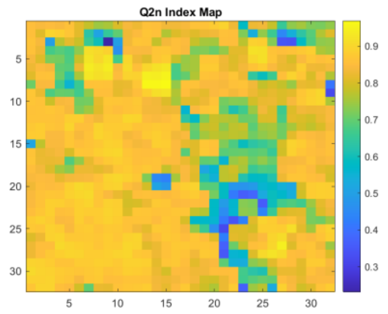

b)

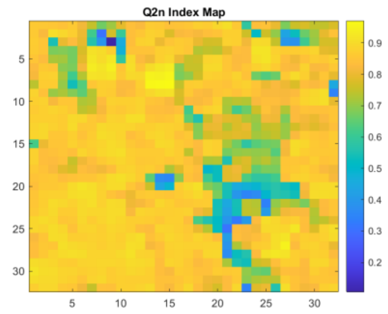

c)

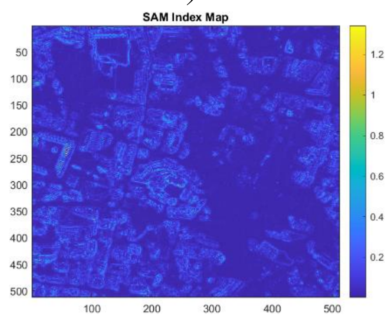

d)

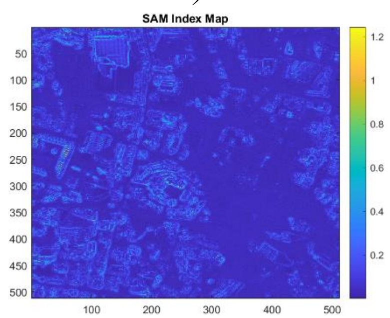

e)

Due to some complex values inside the SAM matrix, the SAM map was not available as a MATLAB output, for the image computed with Brovey.

Two major trends are already visible by looking at the indexes:

1. the HPF algorithm return much better results compared to the other two, although both GIHS and Brovey have good indexes;
2. pansharpening done with images not upscaled have better indexes than the one done with upscaled multispectral images (due to the artefacts analyzed in chapter 2.1.

These two trends, as can be seen in the next pages, will repeat themselves, proving both points just discussed.

4.5 Indexes for the Worldview W4 Mexican nature dataset

As for the London dataset, the indexes computed at reduced resolution, with the IDL-upscaled multispectral image, will be analyzed first.

Algorithm	SAM	ERGAS	Q2N
HPF	2.7996	10.4295	0.8250
Brovey	2.6652	8.2620	0.8247
GIHS	3.1070	8.5544	0.8196

Table 3 - Indexes for Mexican image, fused with MS upscaled

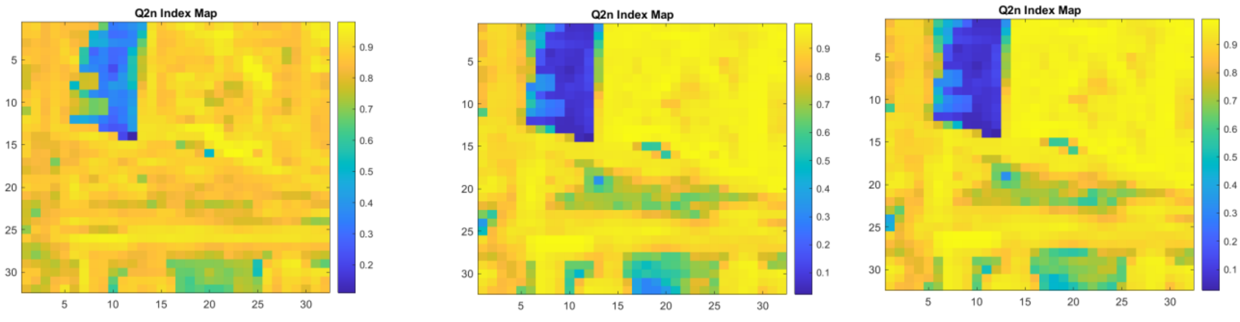

a) *b)* *c)*

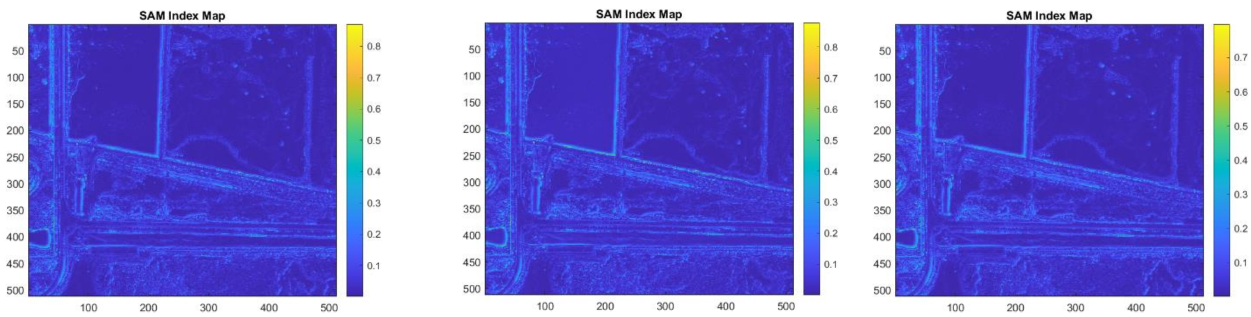

d) *e)* *f)*

In this case, indexes are generally more similar, with the only real difference in the ERGAS index of the HPF function, being a little higher than the other two algorithms. Q2N maps show similar output too, with the worst output being in the field in the top right, for all the algorithms. SAM indexes show instead a general better output, compared to the London urban dataset.

In the next page will be analyzed the indexes and maps of the images fused with reduced resolution, full scale multispectral image.

Algorithm	SAM	ERGAS	Q2N
HPF	2.3726	7.2486	0.8865
Brovey	2.6652	8.2620	0.8247
GIHS	2.5736	7.6655	0.8333

Table 4 - Indexes for Mexican image, fused with same size PAN and MS

The same error as before occurred again in computing the SAM map of the image fused with the Brovey algorithm, so it was not available.

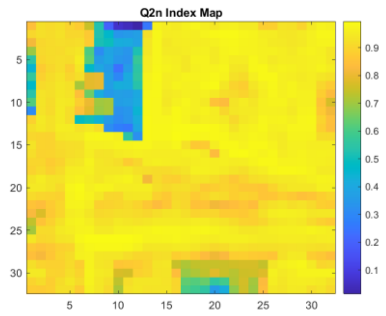

a)

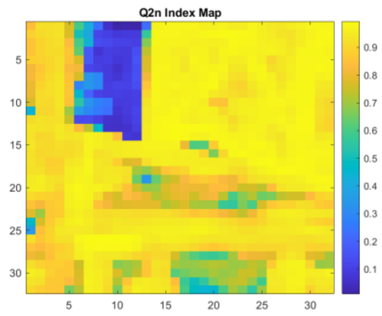

b)

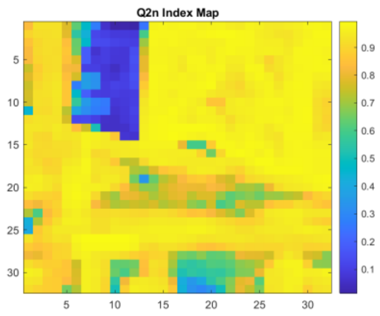

c)

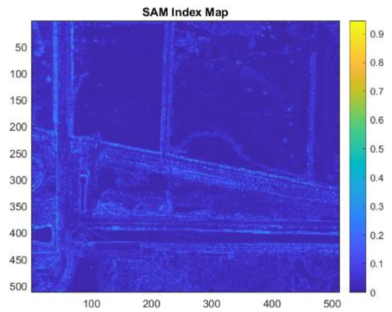

d)

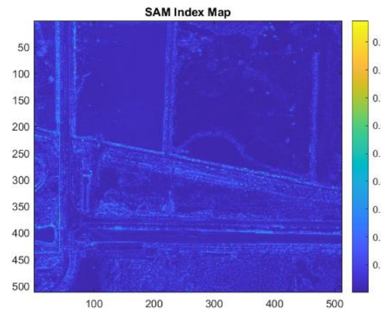

e)

In the case of the Mexican dataset there is not a better algorithm deductible from indexes and maps. All the algorithms, in the nature case, gives very similar output and makes the same mistakes in the same areas. Even the visual comparison does not show clear difference between all the output which seems all almost identical.

4.6 Comparison of indexes

Indexes computed with our algorithm's images has been compared with the indexes computed on the MATLAB output. In the case of GIHS and Brovey, the first indexes were identical compared to the one coming from MATLAB images.
In the case of HPF, instead, indexes computed on the images from our IDL implementations, are much better than those computed on MATLAB output images.
Results are visible in TABLE for the London dataset and in TABLE for the Mexican dataset.

Algorithm	**SAM: M vs IDL**	**ERGAS: M vs IDL**	**Q2N: M vs IDL**
HPF	4.1973 - 4.0003	44.5592 - 25.5388	0.5873 - 0.9133
Brovey	4.1973	31.8140	0.8039
GIHS	4.4847	31.1424	0.8121

Table 5 - Index comparison on the London dataset

Algorithm	**SAM: M vs IDL**	**ERGAS: M vs IDL**	**Q2N: M vs IDL**
HPF	2.2323 - 2.4812	11.8575 - 7.2196	0.7192 - 0.8883
Brovey	2.2323	7.4901	0.8381
GIHS	2.7536	7.6655	0.8333

Table 6 - Index comparison on the Mexican dataset

Brovey and GIHS match exactly the output from MATLAB, having the exact same indexes.
HPF, instead, performs better in every situation, having better indexes compared to MATLAB.

List of figures

List of tables

Bibliography

(1) "*Pansharpening of RASAT and GÖKTÜRK-2 images via High Pass Filter*" by Oya Burcu Bakioğlua, Hüseyin Topana, Mustafa Özendia, Ali Cama

(2) "*Pansharpening Toolbox for Distribution*", presented in the paper "*A Benchmarking Protocol for Pansharpening: Dataset, Preprocessing, and Quality Assessment*", by Gemine Vivone, Mauro Dalla Mura, Andrea Garzelli and Fabio Pacifici.